

Jonathan Nakane¹
Mark Akeson²
Andre Marziali¹

Evaluation of nanopores as candidates for electronic analyte detection

¹Department of Physics and Astronomy, University of British Columbia, Vancouver, BC, Canada

²Howard Hughes Medical Institute and Department of Chemistry, University of California, Santa Cruz, CA, USA

In an effort to increase throughput and decrease the cost of electrophoretic separation of DNA and proteins, various groups are developing highly parallel, miniaturized separation devices based on capillaries etched into silicon, glass or plastic substrates. To date, these miniaturized devices have relied on optical detectors, thus placing a lower limit on instrument size, and complicating the incorporation of an entire DNA analyzer instrument on a chip. To address this limitation, we are evaluating nanopores as candidate Coulter counters for purely electronic detection of analytes in miniaturized electrophoresis and similar separation devices. To establish feasibility of this detection scheme, we have investigated the detection sensitivity of a nanopore sensor through experiments with the α -hemolysin (α -HL) ion channel, and through a Monte Carlo (MC) model of polymer capture rate with a cylindrical nanopore under an applied voltage. Experimental and model results are extrapolated to predict the capture rate of synthetic pores operating at higher voltages than presently achievable with protein pores.

Keywords: Biosensor / DNA sequencing / Miniaturized electrophoresis / Nanopore EL 5087

1 Introduction

1.1 General aspects

In an effort to increase throughput and decrease the cost of electrophoretic separations for DNA sequencing, several groups [1–7] have successfully miniaturized capillary electrophoresis (CE) systems by etching or forming capillaries into glass, silicon, or similar substrates. This has led to the possibility of faster and highly parallel separations on a chip, and the development of commercial instruments such as the Agilent 2100 Bioanalyzer (Agilent, Palo Alto, CA, USA) and the Caliper LabChip (Caliper Technologies, Mountain View, CA, USA). Some of the advantages of miniaturized separation technologies are negated by the bulky laser induced fluorescence (LIF) or UV absorbance optics that are typically used for analyte detection. Furthermore, the quantity of analyte present in the electrophoresis channels must still be sufficient to generate a reasonable optical signal above background electrical noise and fluorescence.

Additional difficulties and costs occur in CE systems with LIF based detection. For example, in DNA sequencing, fluorescent dyes must be incorporated into the DNA fragments to be separated. These dyes both increase the

cost of the sequencing process, and require reaction product purification to remove unincorporated dyes that overlap with analyte bands in the electropherogram and contaminate the separation data. To remove the limitations on CE imposed by optical detection, and to take advantage of the potential miniaturization of capillaries, it is desirable to develop completely electronic detection systems that would be amenable to fabrication on a chip. We are investigating one such strategy in which nanometer scales pores ('nanopores') are used as Coulter counters [8] to electronically detect bands during capillary electrophoresis. The concept of detecting single DNA or RNA molecules using a nanopore was proven [9] using an α -hemolysin (α -HL) ion channel – a protein that self-assembles as a ~ 2 nm diameter pore [10] in lipid bilayers – to detect and characterize individual DNA molecules.

In this approach, DNA molecules are detected as shown in Fig. 1. A single α -HL channel is incorporated into an artificially constructed lipid bilayer separating two buffer reservoirs filled with electrolyte, typically 1 M KCl. A voltage (usually 100–300 mV) is applied across the lipid bilayer, resulting in a ionic current of ~ 90 pA at 100 mV through the α -HL channel. When DNA is introduced into solution near the channel, some DNA molecules are captured by the electric field of the channel and translocate through the channel. During this translocation, the ion current in the channel is reduced by the presence of the DNA. This reduction in current can be detected and, if desired, analyzed to provide some information on the nucleotide composition of the DNA molecule [11, 12].

Correspondence: Andre Marziali, Rm 415, Department of Physics and Astronomy, UBC, 6224 Agricultural Rd, Vancouver, BC, Canada, V6T-1Z1

E-mail: andre@physics.ubc.ca

Fax: +604-822-5324

Abbreviations: α -HL, α -hemolysin; MC, Monte Carlo

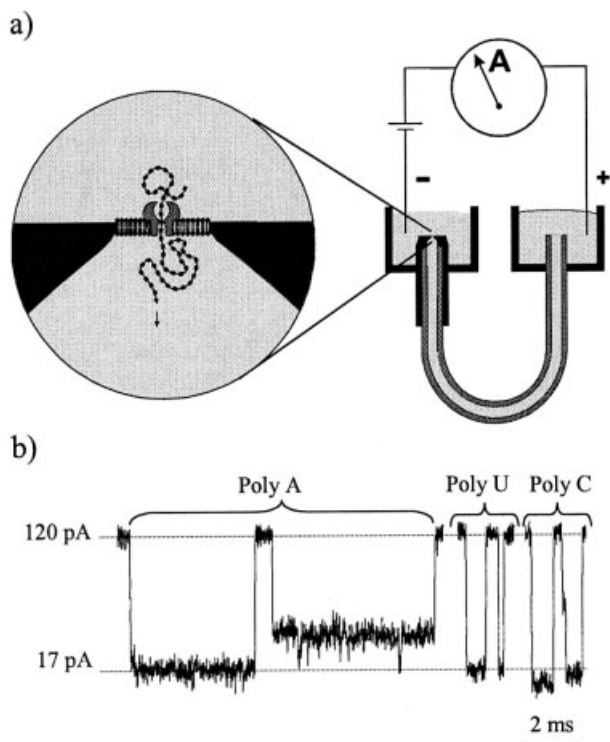


Figure 1. Prototype nanopore device for capture and examination of individual RNA or DNA molecules. (a) Schematic of the device. One α -HL channel is inserted into a horizontal, 25 μm diameter bilayer formed across a conical aperture at the end of a Teflon tube. The Teflon 'patch tube' connects two 200 μL baths. Voltage is applied across the protein channel between two Ag/AgCl electrodes. When DNA is translocated through the channel, ionic current is impeded. (b) Typical ionic current blockades caused by polyA, polyU, and polyC 100-mers [11].

One benefit of a nanopore based analyte sensor is its ability to yield additional information on the molecule being detected, for example, its charge polarity (though probably not its total charge), or its approximate length. Furthermore, an appropriately sized nanopore should be capable of detecting molecules from 10 bp to thousands of bp in length: even if the longer molecules do not translocate through the pore, their interaction with the pore at high applied potentials should still be detectable as a blockage which will persist until cleared by applying a reverse potential (events such as these have been detected with the α -HL channel; data not shown). On a small scale, the nanopore is an extremely sensitive detector, yielding an actual count of molecules in its proximity. Its practical sensitivity will depend on the size of the volume it is intended to sample. Therefore, unlike optical detection schemes, the nanopore sensor will capture an increasing percentage of the total number of molecules and become more efficient as the diameter of the capillary

it is sampling is decreased. Finally, the nanopore detector is a purely electrical system amenable to both the detector and its associated electronics being manufactured on the same chip as the separation capillaries.

Though the α -HL channel is an interesting prototype for a nanopore sensor, it is not robust enough to be used as part of an instrument. A synthetic nanopore will need to be created to make this detection scheme practical. Though that issue is not addressed in this paper, it should be noted that the construction of nanometer sized individual pores in silicon nitride, and detection of DNA strands with such a pore, has been demonstrated [13]. To determine the feasibility of using a nanopore as a CE detector, the sensitivity of the pore as a charged analyte detector must be evaluated, particularly at the higher voltages (> 300 mV) that could be applied to a synthetic pore, as capture rate and detection efficiency are expected to increase with voltage. In order to do this, the capture rate of DNA molecules in the vicinity of the α -HL pore has been measured at the highest voltages we could achieve without rupturing the lipid bilayer containing the pore, and modeled using Monte Carlo (MC) methods at the even higher voltages expected to be practical with synthetic pores. Predictions of capture rates of an ideal synthetic pore are arrived at based on the observed capture behavior of α -HL and the results of the MC computer simulations.

1.2 Nanopore detection of analytes in a CE system

Figure 2 shows the proposed application of a nanopore to band detection in a CE device. A separation capillary is mounted and operated conventionally, with a nanopore fabricated at or near the elution end of the capillary (the anode end in a DNA sequencing system) in such a way that it is exposed to the analyte. While an electrophoretic potential is applied across the main capillary, a smaller capture and detection potential is applied across the nanopore. The flow of buffer ions through the nanopore is monitored continuously.

As bands of charged analyte drift near the nanopore, some of the molecules in closest proximity to the pore will collide with it and possibly translocate or become trapped in the pore. In the latter case, the molecule can be cleared from the pore by reversing the applied voltage. The number of capture events per second should reflect the concentration of charged molecules in the vicinity of the pore. In order to estimate the sensitivity of the nanopore detector it is necessary to measure or estimate the expected rate of detectable blockages (capture rate) as

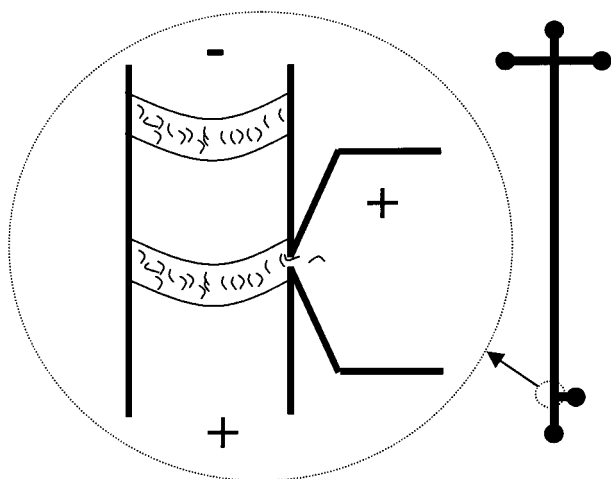


Figure 2. Schematic of proposed separation capillary with nanopore detector (not to scale). Electrophoresis separation potential is applied across the full length of the capillary, while a much smaller capture potential is applied across the pore. Current through the pore is detected and the frequency of events, or capture rate, is plotted as an indicator of local concentration of analyte. As bands of analyte electrophorese past the detector, bursts of events are expected at the nanopore detector. Though the nanopore is shown as fabricated in the capillary wall, it may be more practical to mount the nanopore into a protrusion that locates the pore in the center of the capillary, or to mount the pore in a sheath-flow cell at the elution end of the capillary, thus concentrating the analyte in the vicinity of the pore.

a function of the concentration of analyte molecules. A sense of the dependence of this capture rate on molecule length would also be desirable.

It is also important to measure the voltage dependence of the capture rate and to derive an estimate of this rate for large voltages applied to the pore, though voltages that may be practical for a synthetic pore will likely be too high to measure experimentally with the less robust α -HL pore. Knowledge of this voltage dependence is particularly relevant as there appear to be no published experiments examining the behaviour of the α -HL pore's rate of capture at voltages higher than 150–200 mV. A discussion and computer modeling of molecule capture follows, as well as experimental determination of capture rates.

1.3 Model of molecule capture and detection

DNA capture rates in α -HL channels have been previously measured [14] and fitted with an exponential dependence of molecule capture rate on applied voltage. These measurements were taken in an α -HL channel with single-stranded DNA (ssDNA) concentrations of 400 and 800 nM

of bT-poly(dC)₃₀ at applied voltages ranging from ~ 55 mV to 120 mV. Henrickson *et al.* [14] fit the data to an exponential transition-state relation describing the rate at which molecules overcome an entropic energy barrier to translocate through the channel. The predicted capture rate is:

$$R = R_0 \exp(z e |V| / kT) \quad (1)$$

where the zero-applied-potential capture rate is R_0 , V is the applied potential, and the measured [14] values for R_0 and z are respectively $1.5 \times 10^{-2} \text{ min}^{-1}$ and 1.9 for capture of 400 nM DNA on the *cis* side of the channel. Though this is an excellent fit to the voltage range the authors were interested in, it produces unreasonable results at higher voltages. At 300 mV applied voltage, the predicted capture rate from Eq. (1) is $\sim 10^6 \text{ Hz}$ – several orders of magnitude greater than what is measured. Our experimental measurements (see Section 3) indicate that the exponential dependence of capture rate on voltage cannot be valid much beyond the voltage range over which the measurements were taken (55–120 mV) and a different model of the capture rate will be needed for higher voltages.

We hypothesize that the total capture rate $R(V)$ is the product of the collision rate of molecules with the pore at a given voltage $R_0(V)$, and the probability $P(V)$ that a given molecule will be captured during its interaction with the pore at this voltage: $R(V) = R_0(V) * P(V)$. For voltages $V > V_0$, where V_0 is the lowest voltage at which $P(V_0) \sim 1$ at the entrance of the pore, we hypothesize that the capture rate can be modeled strictly as diffusive collision of the analyte with an imaginary hemispherical surface defining a region near the pore beyond which molecules may not escape capture. We make analytical estimates for the collision rate $R_0(V)$ and its dependence on applied voltage V , and use a MC simulation to predict the likelihood of capture $P(V)$ for each collision.

1.4 Estimate of molecule collision rate with pore

The term “collision” in a diffusive process is well defined in the case of point-like particles diffusing towards a perfectly adsorbing pore [15] but is somewhat poorly defined in the case of a reflecting or not perfectly adsorbing pore. Our estimate for diffusive collision rate will therefore be split into two voltage regimes: above and below the voltage V_0 required for certain capture. For voltages above V_0 defined such that $P(V_0) \sim 1$ and the pore is a perfect adsorber, we can define a capture radius $r(V)$ as the minimum distance from the pore at which molecules may escape capture. On the hemispherical surface defined by this radius, $P(V) = 1$. We can then produce a well-

defined estimate for the collision rate, which in this case is equal to the capture rate, by considering this hypothetical surface to be a perfect adsorber. In this limit the capture rate is purely determined by the diffusive process with field induced drift. The MC simulation of molecule capture will yield an estimate for the value of V_0 for a ssDNA chain of specific length (see Section 3).

In the case where a substantial fraction of molecules come in contact with the pore and diffuse away from the pore without being captured, the definition of collision rate becomes dependent on the arbitrary distance from the pore beyond which a molecule is defined as having escaped. Following Berg's arguments [15] that diffusing molecules are not aware of their past, we estimate the collision rate with the pore to be comparable to the capture rate of a perfectly adsorbing disc of similar size to the pore. By this estimate, the collision rate without applied voltage is

$$R_0 = 4CDa \quad (2)$$

where C is the molecule concentration, D is the diffusion constant for the molecule, and a is the radius of the disc.

One might consider that applying a voltage across the pore will produce an electric field in the vicinity of the pore that will tend to attract molecules and increase the collision rate above that estimated in Eq. (2). This turns out to not be the case for our parameters, as the pore size is of the same size scale as the molecules attracted to the pore. An estimate for the field induced collision rate of point particles attracted to an adsorbing disc is normally arrived at through a solution of the diffusion equation with drift [16]. In spherical coordinates, and assuming azimuthal symmetry:

$$D \frac{1}{r^2} \frac{\partial}{\partial r} \left(r^2 \frac{\partial C}{\partial r} \right) + \mu \frac{1}{r^2} \frac{\partial}{\partial r} (r^2 EC) = \frac{\partial C}{\partial t} \quad (3)$$

where the first term is the diffusion equation, and the second term describes motion of a charged molecule with mobility μ in an electric field E . To show that field-induced concentration gradients do not play a role in the determination of the collision rate, we have implemented a numerical solution of this equation for hypothetical point particles with concentration boundary conditions $C(\text{inf}) = C_0$ (the bulk molecule concentration) and $C(r < 1 \text{ nm}) = 0$, implying that molecules within 1 radius of the pore are captured by the pore. The electric field in the vicinity of the pore is calculated based on the expected current density in the pore by considering Ohm's law ($J = \sigma E$), the continuity equation for electric current ($\int \vec{J} \cdot d\vec{A} = 0$), and the boundary condition for current at the interface with an insulating material ($J_{\perp} = 0$). The solution to these equations outside the pore (on either side of a cylindrical

channel) is analogous to the electrostatic field solution in the vicinity of a thin disc of charge. Taking advantage of this similarity and performing appropriate variable substitutions yields the on-axis current-induced field near the pore:

$$E \cong E_0 \left(1 - \frac{r}{\sqrt{r^2 + a^2}} \right) \quad (4)$$

where a is the approximate radius of the channel (1 nm for α -HL), and r is the distance from the center of the pore. It is important to note that this solution is the current-induced field and not an electrostatic field. We have neglected any electrostatic interactions based on the fact that the Debye length in our experimental conditions (1 M KCl) is only 0.3 nm. All electrostatic fields will therefore be screened within a distance shorter than the length scale of the error between the actual pore geometry and our simplified geometric representation of the pore. E_0 in Eq. (4) is derived from the applied potential by the approximation

$$V = \int_{-\infty}^{\infty} E dr = E_0(L + 2a) \quad (4a)$$

where L is the length of the channel (10 nm for α -HL), which implies that the electrical impedance of the simplified channel is dominated by the length of the channel itself plus the channel access resistance (of the order of one channel radius) on each side of the channel. Macroscopic finite element calculations based on this geometry confirm this as a reasonable approximation.

A numerical solution to Eq. (3) ($V = 200 \text{ mV}$, $C = 1 \mu\text{M}$, $\mu = 2 \times 10^{-8} \text{ m}^2/\text{Vs}$ [17], $D = 5 \times 10^{-11} \text{ m}^2/\text{s}$ [17]), indicates that the scale of the field induced concentration gradient is on the order of the size scale of the pore (1 nm). As the molecules of interest in this experiment are of the same size scale as the entire extent of the predicted gradient, we confirm that Eq. (3) is not applicable in this case and that consequently the concentration of molecules in the vicinity of the pore is not affected by the weak electric field resulting from electric current density in the pore. We will therefore model the collision rate based on a perfectly adsorbing channel subject only to diffusive flux of molecules from the surrounding solution. For voltages below V_0 , we derive the predicted event rate by adjusting the estimated collision rate with the pore entrance by the predicted likelihood of capture $P(V)$. Above V_0 , we will treat the perfect adsorber as an imaginary surface on which $P(V) = 1$. For $V > V_0$, this surface will extend beyond the channel entrance due to higher electric field.

A crude estimate of the voltage dependent maximum radius $r(V)$ at which $P(V) \sim 1$ (i.e., the surface of the hypothetical perfect adsorber) can be made by considering

that the capture radius of the pore is proportional to the distance at which the electrophoretic drift velocity of a DNA molecule is comparable to the average diffusion velocity over that same distance scale. The average diffusion velocity v_{diff} for motion in the radial dimension over a length scale r is approximately

$$v_{\text{diff}} = \frac{2D}{r} \quad (5)$$

The electric field a distance r on-axis outside the pore is given by Eq. (4). For a distance r greater than twice the radius a ,

$$E \approx \frac{E_0 a^2}{2r^2} \quad (6)$$

is a reasonable approximation both on- and off-axis. The field-induced velocity is:

$$v_e = \mu E \quad (7)$$

where μ is the mobility of the molecule. Setting these two velocities to be equal at radius r , and assuming $r > 2a$, the capture radius can be written as:

$$r(V) \propto \frac{\mu a^2}{4D} E_0 \quad (8)$$

The capture rate of a perfectly adsorbing hemisphere of radius r [15] in the presence of a bulk concentration C of the molecule being captured is given by:

$$R = 2\pi C D r \quad (9)$$

Therefore, in the regime above V_0 , we can estimate the collision rate and overall capture rate to be:

$$R \propto a^2 C \mu E_0 \quad (10)$$

In summary, we expect the total capture rate as a function of voltage to be:

$$\begin{aligned} R &= 4CDa^*P(V) & V < V_0 \\ R &= 4CDa & V \sim V_0 \\ R &\propto a^2 C \mu \frac{V}{(L+2a)} & V \gg V_0 \end{aligned} \quad (11)$$

It is likely that other effects may limit the capture rate within this regime. For example, the finite lifetime of the translocation events (10's to 100's of μs) will limit the capture rate at higher concentrations and voltages, as molecules can only enter the pore one at a time. In this limit, the capture rate will no longer depend linearly on the concentration and interaction between molecules will need to be considered. A conservative estimate for this limit is a few kHz (1/100's μs) – well beyond the range of our experimental and expected operating conditions.

1.5 Probability of molecule capture at low voltages

For the purpose of this investigation, we are interested in predicting the approximate behavior of $P(V)$ at voltages below V_0 , and in predicting the value of V_0 . Some understanding of how $P(V)$ varies with N , the length of the molecule measured in Kuhn lengths, would also be desirable. To achieve this, we have generated a simple MC simulation of a charged polymer in the vicinity of a reflecting wall containing a cylindrical pore (radius 1 nm, length 10 nm) and subject to both random thermal motion and electric field induced drift. The polymer is represented as a pearl-necklace chain of N hard beads freely jointed by rigid links of length b (1.5 nm – one Kuhn length for ssDNA in high ionic strength buffers [18]). N is therefore $N = n/3$ where n is the number of nucleotides in the ssDNA strand being modeled. Hard-wall interactions constitute the boundary conditions at the wall and in the interior of the pore. For simplicity, the chain is not forced to be self-avoiding though self-avoidance is enforced explicitly on entering the pore by disallowing any bead from entering the pore unless (i) the pore is empty and the bead is an end bead, or (ii) an adjacent bead is already in the pore. Adding self-avoidance to the code produced little change in the capture behavior, presumably as the energetically important interactions are occurring primarily in the pore where self-avoidance is explicitly enforced by the pore geometry. The electric field from the pore is modeled as per Eq. (4) outside the pore, and as $E_0 = \frac{V}{(L+2a)}$ inside the pore. See Section 2 for more details on the simulation.

1.6 Effect of electrophoretic field on capture rate

The use of a nanopore as a detector in a capillary electrophoresis instrument will require blockage events to occur in the presence of an electrophoretic field that is in a direction orthogonal to the axis of the channel. The effect of this field on the capture rate is likely to be insignificant. Typically electrophoresis fields are on the order of $E_z \sim 10^4$ V/m. Using Eq. (6), the pore field and electrophoretic field will be of similar magnitude at a distance of ~ 65 nm from the pore for an applied voltage of $V = 1$ V. As this is much farther than the expected capture radius (a few nanometers), the electrophoretic field is not likely to be a contributing factor for capture rate.

2 Materials and methods

2.1 Polynucleotide detection

The procedure for reconstituting α -HL into a lipid bilayer membrane for polynucleotide detection has been described in detail previously [11]. In summary, horizontal

bilayers were formed at the end of a Teflon tube with a 20 μm hole formed at one end. The tube was inserted into a machined Teflon block with a 200 μL buffer chamber at each end of the tube. The hole was coated in a solution of diphytanoyl phosphatidylcholine (Avanti Polar Lipids, Alabaster, AL, USA) in hexane and allowed to dry under vacuum. The tube and chambers were then filled with a buffer composed of 1.0 M KCl with 10 mM HEPES free acid at a pH of 8.0. A single bristle brush was dipped into diphytanoyl phosphatidylcholine wetted in 1-hexadecene. The lipid was then brushed across the aperture and a 5 mV 60-Hz square wave was applied as a seal test. Approximately 0.1 μg of α -HL (Calbiochem, San Diego, CA, USA) in buffer solution was added to the *cis* side of the bilayer. Once a channel was inserted, the chamber was flushed with buffer to prevent multiple channels from forming. Ionic current was measured using an Axopatch 200B patch clamp amplifier (Axon Instruments, Foster City, CA, USA) and recorded using a NI-MIO-16E-4 National Instruments data acquisition card (National Instruments, Austin, TX, USA). Data was either low-pass filtered by the amplifier unit at 10 kHz, and acquired externally at 50 kHz, or low-pass filtered by the amplifier unit at 100 kHz and acquired externally at 333 kHz, then digitally low-pass filtered at 50 kHz.

For these experiments, the polynucleotides used were homopolymers of poly(dA)₅₀ and poly(dA)₁₀. All samples were ammonia-butanol purified with no further purification steps. Anywhere from 2 to 10 μL of a 40 μM polynucleotide stock solution was added to the 200 μL chamber, mixed by reflux, and allowed to diffuse for 5 min. Data were then acquired for various voltage settings across the channel. All experiments were carried out at 20.0 \pm 0.5°C. An average of \sim 500 capture events were recorded at each concentration and voltage. For each voltage setting, the acquired data was analyzed for events, which were defined as follows: the start of an event occurred when the measured current dropped to less than 80% of the mean open-channel current, and the end of an event occurred when the measured current became equal to or greater than the mean open-channel current. This hysteresis in measuring the start and end time of the event prevented noise during a single event to be counted as several individual events. The frequency of events was taken as the inverse of the mean time duration from the end of one event to the beginning of the next event. In this way, the actual time taken for the duration of each event was excluded.

2.2 MC simulation

An MC simulation of DNA capture by a cylindrical pore was performed by modeling random thermal motion and field-induced drift of a chain of beads linked by freely

jointed rigid rods. Each bead represents one Kuhn length of the ssDNA molecule (approx. 3 nucleotides, 1.5 nm between beads [18]). During each time step τ of the simulation, each bead is displaced a distance $\sqrt{N}\delta$ in a random direction, where δ is the average step size in three dimensions for the molecule's center of mass $\delta = \sqrt{6D\tau}$. Subsequently, each bead is displaced by a distance $\mu\tau\mathbf{E}(r)$ where $\mathbf{E}(r)$ is the electric field vector at the bead's position as calculated using Eq. (4), and μ is the mobility of the DNA molecule in similar ionic conditions. The dimensions of the cylindrical pore were taken to be 2 nm in diameter and 10 nm in length. Approximate values for D and μ were taken to be $5 \times 10^{-11} \text{ m}^2/\text{s}$ and $2 \times 10^{-8} \text{ m}^2/\text{Vs}$, respectively [17]. After the aforementioned displacements are applied to the beads, boundary conditions were applied to reflect the beads from the hard wall and the interior walls of the cylindrical pore. Following the reflection, a position correction was added to each bead simultaneously to constrain the distance between beads:

$$\Delta\vec{r}_i = \frac{1}{2} \left[(\vec{r}_{i-1} - \vec{r}_i) \left(1 - \frac{d}{|\vec{r}_{i-1} - \vec{r}_i|} \right) + (\vec{r}_{i+1} - \vec{r}_i) \left(1 - \frac{d}{|\vec{r}_{i+1} - \vec{r}_i|} \right) \right] \quad (12)$$

where $d = 1.5 \text{ nm}$ is the bead-to-bead distance. The bead radius is 0.7 nm and a typical value of $\tau = 25 \text{ ps}$. Simple tests including measurement of center of mass motion and end-to-end distance of the molecule were performed to test the simulation. The simulations presented in this paper were also run with widely varying values of τ to ensure that there is no dependence of the solution on the arbitrary step size.

Calculations of capture rate were performed by initiating a simulation with a thermally equilibrated DNA molecule in contact with the pore (defined as any one bead contacting the pore surface at the opening). From this point, the simulation ran until either the center of mass of the molecule emerged from the trans side of the pore (a capture event), or the center of mass diffused farther than 15 nm from the pore opening. This "escape distance" was picked arbitrarily to limit computation time. The capture probability $P_{\text{MC}}(V)$ is the number of simulations that result in translocation, divided by the total number of simulations at a given voltage. The total capture probability $P(V)$ (defined as the probability that the molecule will be captured in the limit that the escape distance is infinite) is only slightly greater than the probability $P_{\text{MC}}(V)$ observed from the MC simulation with finite escape distance and can be derived using arguments from Berg [15]. The probability that a molecule released at radial distance b from the pore will approach the pore as close as radial distance a before wandering away to infinity is [15]:

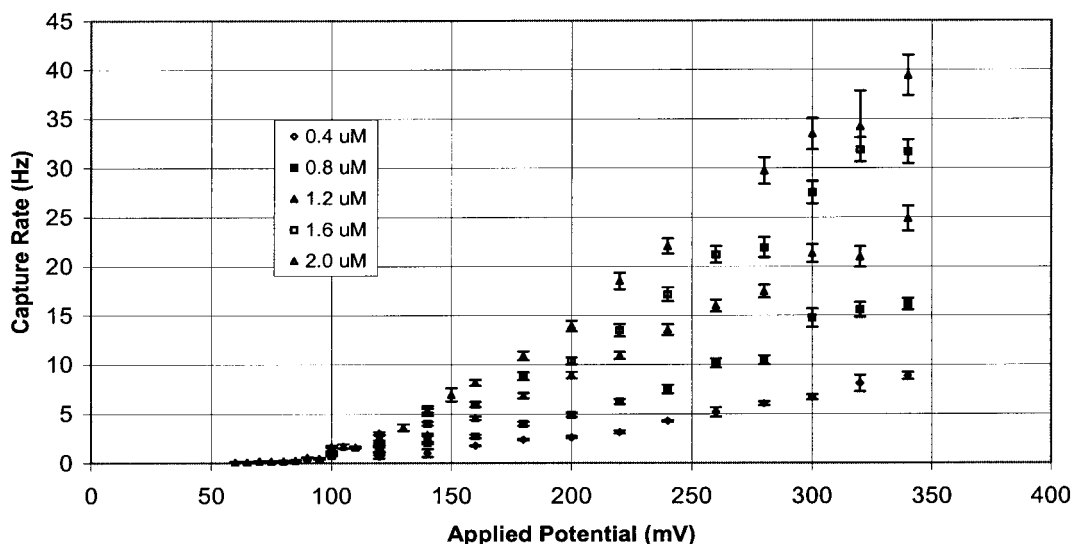


Figure 3. Measured capture rate as a function of voltage applied to pore for various concentrations of ss poly(dA)₅₀ in 1 M KCl. Data below 100 mV was only taken at 2 μ M concentration.

$$\rho = a/b \quad (13)$$

The probability that the molecule starting at a will be captured before drifting as far as b is the value measured by the MC simulation, $P(V)$. The total capture probability can therefore be expressed as:

$$P(V) = \sum_{n=0}^{\infty} (1 - P_{MC}(V))^n \rho^n P_{MC}(V) \quad (14)$$

where $(1 - P_{MC}(V))^n \rho^n$ is the probability that the molecule will make n trips from b to a without being captured or drifting away to infinity. In the infinite limit, this reduces to:

$$P(V) = \frac{P_{MC}(V)}{1 - \rho(1 - P_{MC}(V))} \quad (15)$$

All MC results have been scaled according to Eq. (15) to remove any dependence on the arbitrary escape distance used during the simulation.

3 Results and discussion

Measurements of current blockages and capture rates for two different polymers were performed as described above at different voltages and concentrations. Figure 3 shows a plot of capture rate as a function of voltage and concentration for poly(dA)₅₀ for data acquired at 50 kHz. There was no significant difference in the measured event rates for the poly(dA)₅₀ molecule when the measured current was acquired and analyzed at 333 kHz – for example, at 260 mV, sampling at 50 kHz and 333 kHz resulted in measured event rates of 10.2 \pm 0.3 Hz and 10.6 \pm 0.4 Hz respectively. This is not surprising based on the algorithm used to detect events (see Section 2). We have

defined an event as a 20% drop in the mean open channel current. A typical poly(dA)₅₀ blockage produces an 85% drop in the open channel current [11]. It is therefore reasonable that we can suffer a decrease in blockage amplitude to 20 percent/85% = 24% of the original blockage amplitude and still detect the event with the algorithm presented in this paper. The effect of a 10 kHz low pass filter is to broaden short pulses in time while decreasing their amplitude. Numerical calculations of the 10 kHz 4-pole Bessel filter (not shown) show that a 15 μ s pulse passing through the filter decreases in amplitude to 25% of the original pulse height, and broadens the pulse to a width of 50 μ s. This implies that pulses as short as 15 μ s will be detected as events when filtered through either the 100 kHz or 10 kHz filter. Furthermore, the broadening of the pulse width to 50 μ s ensures that the pulse will not be missed by the 50 kHz sampling frequency used in conjunction with the 10 kHz filter. According to the blockade duration histogram for poly(A)₁₀₀ at 120 mV taken by Meller *et al.* [12], and assuming that the blockade duration increases linearly with the polymer length and decreases with the square of the applied potential [19], we expect that the most frequently occurring value of blockade duration resulting from poly(dA)₅₀ at 240 mV is \sim 40 μ s. Using the distribution of translocation times found by Meller *et al.* [12], we estimate that less than 1% of poly(dA)₅₀ events will be missed for our experimental conditions even when filtering at 10 kHz. An exponential relationship between the applied potential and capture rate at low voltage ($<$ 100 mV), as observed by Henrickson *et al.* [14], was confirmed with data obtained at a poly(dA)₅₀ concentration of 2 μ M (calculations not shown). It is clear from these measurements that the expected low voltage

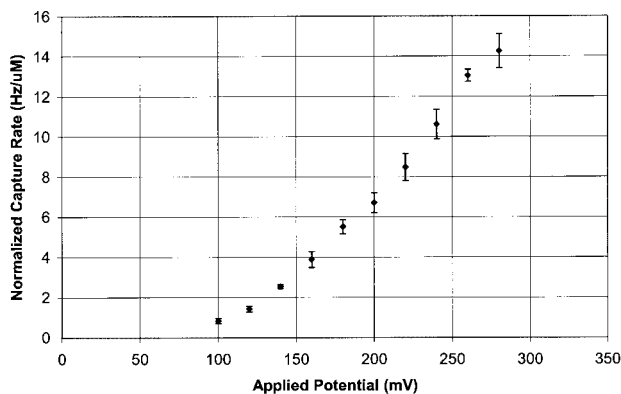


Figure 4. Measured capture rates as a function of applied potential for poly(dA)₅₀ normalized by concentration.

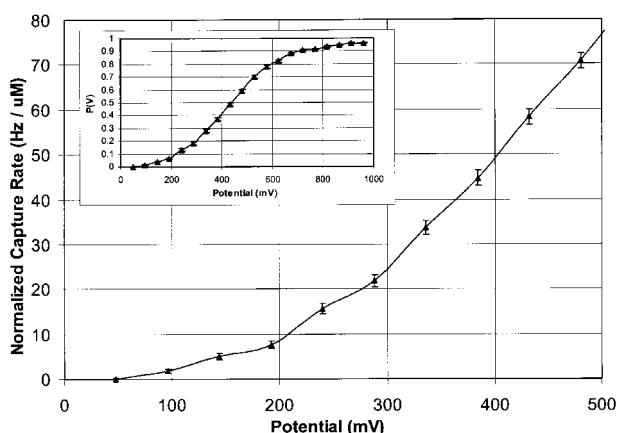


Figure 5. Results of MC simulation of a 50-mer translocating through a cylindrical pore. Capture rate is derived from the calculated capture probability $P(V)$ (inset) by scaling with the expected collision rate $R_0 = 4DCa$. The value of D was chosen to be $D = 5 \times 10^{-11} \text{ m}^2/\text{s}$, yielding a theoretical rate of molecule collision with the mouth of the pore to be $120 \text{ Hz}/\mu\text{M}$. It should be noted that though the capture probability $P(V)$ must saturate at $P(V) = 1$, this will not result in saturation of the actual capture rate as the radius of the capture hemisphere will expand beyond the size of the pore at voltage beyond this limit. For this reason we have limited the calculation of capture rate to voltages for which the capture probability is well below 1.

exponential dependence of capture rate on voltage terminates at approximately 150 mV, with further increases in voltage above this threshold resulting in an approximately linear increase in capture rate.

Concentration dependence of the capture rate appears linear as previously reported [14]. To combine data at different concentrations, the frequency data for each set was normalized to a concentration of $1 \mu\text{M}$ by dividing the measured capture rate by the concentration. The

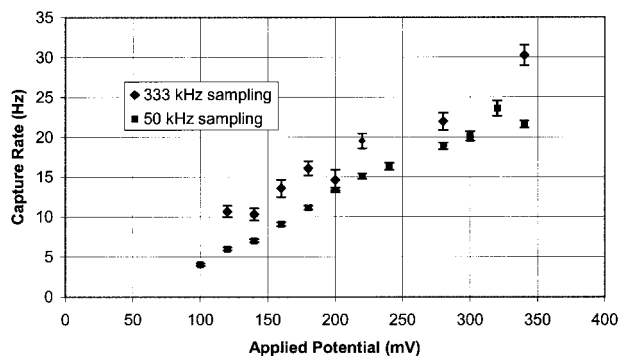


Figure 6. Measured capture rate of $0.4 \mu\text{M}$ poly(dA)₁₀ in the α -HL channel acquired at 333 kHz with 100 kHz low-pass analog filtering and 50 kHz lowpass digital filtering, and at 50 kHz with 10 kHz lowpass analog filtering.

data sets for the same polymer at various concentrations were averaged at each value of applied voltage to obtain the combined data plotted in Fig. 4. Error bars denote the experimental variability as assessed by the multiple measurements of capture rate for the same molecule with different concentrations.

Figure 5 presents the results of the MC simulation of DNA capture. The calculated capture probability $P(V)$ was converted to capture rate by scaling the probability by the expected collision rate $R_0 = 4DCa$. The spatial step-size in the MC simulation was $\delta = \sqrt{6D\tau}$. The value of D was chosen to be $D = 5 \times 10^{-11} \text{ m}^2/\text{s}$. This appears to be a reasonable value when compared to measured values of D ($\sim 6 \times 10^{-11} \text{ m}^2/\text{s}$ [17]) for a similar polymer albeit in a different buffer. The simulation results presented in Fig. 5 indicate a similar behavior to the measured capture rates, with an initially rapid increase in capture rate at low voltages, followed by an approximately linear increase for voltages above ~ 100 – 200 mV. Based on the simulation, the value of V_0 is estimated to be ~ 1 – 1.5 V for a 50-mer of DNA in the experimental conditions stated above. We therefore expect the hypothetical event rate at 1 V to be equal to the collision rate: $\sim 100 \text{ Hz}/1 \mu\text{M}$ for this molecule. Since the voltage regime of the experiments is well below the value of V_0 , all of the experiments described here fall into the region described by the first equation in Eqs. (11).

Measurements of capture rate as a function of voltage were also made using the shorter polymer poly(dA)₁₀ at $0.4 \mu\text{M}$ concentration. The data acquired at 50 kHz and 333 kHz for the poly(dA)₁₀ polymer are shown in Fig. 6. It was found that for the shorter polymer, there was a difference in the event rate between data filtered at 10 kHz and 100 kHz, with the latter indicating a higher capture rate. A likely cause for this discrepancy is that a fraction of the blockage events resulting from poly(dA)₁₀ translocation

were too short in duration to be detected with the 10 kHz filter. In spite of the missed events with 10 kHz filtering, and possibly events missed with 100 kHz filtering, both the MC simulation (not shown) and the experimental data indicated higher capture rates for the shorter poly(dA)₁₀ polymer as compared to the poly(dA)₅₀. This finding is in accordance with previous studies with polymer translocation through nanopores [9]. At 300 mV applied voltage and 0.4 μM molecule concentration, the measured capture rate for poly(dA)₅₀ is 6.7 Hz, while the measured capture rate for poly(dA)₁₀ at 10 kHz filtering in the same conditions is 20.1 Hz despite any missed events.

Assuming a synthetic nanopore can be produced from a material such as SiO₂ or Si₃N₄ with dielectric breakdown fields greater than 1×10^8 V/m, it should be possible to achieve electric fields at the opening of the pore comparable to those that would be present in α-HL at voltages ~ 500 mV if the biological channel could withstand these fields. Measurement of current versus voltage for α-HL (data not shown) indicate that current is linear with voltage up to at least 340 mV, and though this linearity may extend up to 1 V and beyond in a synthetic channel, we will limit our estimates to 500 mV as it is possible that there will be limits imposed by thermal dissipation within a synthetic pore to prevent higher voltages from being employed. Extrapolating the measured event rate for poly(dA)₅₀ to the above estimate for the maximum potential we can apply to the pore, we can predict the maximum capture rate of molecules similar to poly(dA)₅₀ to be ~ 40 Hz/μM. The MC simulation predicts a capture rate at 500 mV of ~ 0.6 times that achieved by a perfectly adsorbing disc: $R = 0.6(4CDa)$ or ~ 75 Hz/μM concentration.

We can now predict the sensitivity of the nanopore for molecules similar in size to the 50-mer used for these experiments. A typical spontaneous gating rate for the α-HL channel with no DNA molecules present is 0.3 events/s (not shown). Using this as a noise estimate, the capture rate necessary to achieve both a sufficient signal-to-noise ratio and adequate event statistics for electrophoresis band detection would be approximately 10 events/s. Based on the experimental results presented in Fig. 4, the required concentration of 50-mers in the vicinity of the pore to achieve this capture rate is ~ 250 nM. Even for conventional capillary electrophoresis parameters (ABI 310; 50 μm ID capillary, 1–1.5 mm typical band length) this results in a need for ~ 2.5×10^8 molecules per band, a comparable value to the estimated operating concentration of commercial CE sequencing systems. The detection efficiency of the nanopore sensor will increase with decreasing capillary diameter, for example only requiring 2.5×10^6 molecules per band for a 5 mm ID capillary.

4 Concluding remarks

We have used ssDNA capture by the α-HL channel to test the feasibility of nanopores as sensors for capillary electrophoresis. In particular, the capture rate in the previously unexplored regime above 150 mV appears to be approximately linear rather than exponential as a function of voltage. A simple MC simulation shows similar behavior in this voltage regime. Based on a simulation for ssDNA polymers approximately 50 nucleotides in length analyzed at 500 mV applied potential, we should expect capture rates on the order of 40 Hz for each 1 μM of molecule concentration. Longer molecules may result in lower capture rates for a given size pore, indicating that a practical detection system may require multiple pore sizes to be employed to detect a large range of molecular lengths. Because the nanopore samples a very limited volume, it should be more efficient in conjunction with smaller capillaries than are optical detectors. This scaling property suggests that a durable synthetic nanopore would be particularly suitable for further miniaturization of CE and for incorporation of CE on a chip.

This work is funded in part by the Natural Sciences and Engineering Research Council of Canada (NSERC) and by the Howard Hughes Medical Institute(MA). We thank Steven Plotkin for his assistance and helpful discussions, and Wenonah Vercoutere for help with the α-HL experiments.

Received December 21, 2001

5 References

- [1] Liu, S., Shi, Y., Ja, W. W., Mathies, R. A., *Anal. Chem.* 1999, 71, 566–573.
- [2] Shi, Y., Simpson, P. C., Scherer, J. R., Wexler, D., Skibola, C., Smith, M. T., Mathies, R. A., *Anal. Chem.* 1999, 71, 5354–5361.
- [3] Schmalzing, D., Tsao, N., Koutny, L., Chisholm, D., Srivastava, A., Adourian, A., Linton, L., McEwan, P., Matsudeira, P., Ehrlich, D., *Genome Res.* 1999, 9, 853–858.
- [4] Salas-Solano, O., Schmalzing, D., Koutny, L., Buonocore, S., Adourian, A., Matsudeira, P., Ehrlich, D., *Anal. Chem.* 2000, 72, 3129–3137.
- [5] Koutny, L., Schmalzing, D., Salas-Solano, O., El-Difrawy, S., Adourian, A., *Anal. Chem.* 2000, 72, 3388–3391.
- [6] Backhouse, C., Caamano, M., Oaks, F., Nordman, E., Carrillo, A., Johnson, B., Bay, S., *Electrophoresis* 2000, 21, 150–156.
- [7] Liu, S., Ren, H., Gao, Q., Roach, D. J., Loder, R. T. Jr., Armstrong, T. M., Mao, Q. L., Blaga, J., Barker, D. L., Jovanovich, S. B., *Proc. Natl. Acad. Sci. USA* 2000, 97, 5369–5374.
- [8] Bezrukov, S. M., *J. Membrane Biol.* 2000, 174, 1–13.
- [9] Kasianowicz, J. J., Brandin, E., Branton, D., Deamer, D. W., *Proc. Natl. Acad. Sci. USA* 1996, 93, 13770–13773.

- [10] Song, L., Hobaugh, M. R., Shustak, C., Cheley, S., Bayley, H., Gouaux, J. E., *Science* 1996, 274, 1859–1866.
- [11] Akeson, M., Branton, D., Kasianowicz, J. J., Brandin, E., Deamer, D. W., *Biophys. J.* 1999, 77, 3227–3233.
- [12] Meller, A., Nivon, L., Brandin, E., Golovchenko, J., Branton, D., *Proc. Natl. Acad. Sci. USA* 2000, 97, 1079–1084.
- [13] Li, J., Stein, D., McMullan, C., Branton, D., Aziz, M. J., Golovchenko, J. A., *Nature* 2001, 412, 166–169.
- [14] Henrickson, S. E., Misakian, M., Robertson, B., Kasianowicz, J. J., *Phys. Rev. Lett.* 2000, 85, 3057–3060.
- [15] Berg, H. C., *Random Walks in Biology*, Princeton University Press, Princeton 1983.
- [16] Schumaker, M. F., Kentler, C. J., *Biophys. J.* 1998, 74, 2235–2248.
- [17] Nkodo, A. E., Garnier, J. M., Tinland, B., Ren, H., Desruisseaux, C., McCormick, L., Drouin, G., Slater, G. W., *Electrophoresis* 2001, 22, 2424–2432.
- [18] Smith, S. B., Cui, Y., Bustamante, C., *Science* 1996, 271, 795–799.
- [19] Meller, A., Nivon, L., Branton, D., *Phys. Rev. Lett.* 2001, 86, 3435–3438.